

Electronic Supplementary Information

Monodispersed Plasmonic Prussian Blue Nanoparticles for Zero-background SERS/MRI-guided Phototherapy

Wei Zhu,^a Meng-Yue Gao,^a Qing Zhu,^{*b} Bin Chi,^c Ling-Wen Zeng,^{*d} Ji-Ming Hu,^a and Ai-Guo Shen^{*a,e}

^a College of Chemistry and Molecular Sciences, Wuhan University, Wuhan 430072, China.

^b Department of Neurology, Union Hospital, Tongji Medical College, Huazhong University of Science and Technology, Wuhan 430022, China. E-mail: xhzhuqing@126.com

^c Department of Radiology, Union Hospital, Tongji Medical College, Huazhong University of Science and Technology, Wuhan 430022, China.

^d Institute of Environment and Safety, Wuhan Academy of Agricultural Science, Wuhan 430207, China. E-mail: zeng6@yahoo.com

^e School of Printing and Packaging, Wuhan University, Wuhan 430079, China. E-mail: agshen@whu.edu.cn

Experimental Procedures

Reagents and Materials. Gold(III) chloride trihydrate ($\text{HAuCl}_4 \cdot 3\text{H}_2\text{O}$, 99%), sodium citrate (99%), potassium ferricyanide ($\text{K}_3[\text{Fe}(\text{CN})_6]$, 99%), potassium ferrocyanide ($\text{K}_4[\text{Fe}(\text{CN})_6]$, 99%), ferric chloride hexahydrate ($\text{FeCl}_3 \cdot 6\text{H}_2\text{O}$, 99%), Poly-L-Lysine (PLL, 10%), 1-Ethyl-3-(3'-dimethylaminopropyl) carbodiimide (EDC), N-Hydroxysuccinimide (NHS), hyaluronic acid (HA, 4000 Da), 3-(4,5-dimethyl-2-thiazolyl)-2,5-diphenyl-2-Htetrazolium bromide (MTT), dimethyl sulfoxide (DMSO), hydrogen peroxide (H_2O_2 , 30%) were purchased from Aladdin industrial corporation. Cetyltrimethyl ammonium bromide (CTAB), 3,3',5,5'-tetramethylbenzidine (TMB) dihydrochloride, 2,2,6,6-tetramethyl-4-piperidone (TMPD), were purchased from Sinopharm Chemical Reagent CO., Ltd. All involved antibodies were purchased from Abcam. All of the chemicals were analytical grade and used without further purification, Milli-Q water (18.2 $\text{M}\Omega \cdot \text{cm}$, Millipore) was used throughout this work.

Synthesis of Au NPs. Firstly, Au NPs were synthesized by the citrate reduction method, 100 mL deionized water containing 1 mL of 1% HAuCl_4 was heated to slight reflux with vigorous stirred at 125 °C, then 1 mL of 1% trisodium citrate was subsequent added into the mixture. The color of mixture solution changed from colorless to red and then kept at 125 °C for another 20 min. After the reaction, the system was naturally cooled down to room temperature.

Synthesis of Au@PB NPs. Au@PB core shell NPs were synthesized by using the Liu et al developed method with a slight change. Two steps were included for this aim, first, Au@CN- NPs were prepared, which 19 mL of the above gold colloid was etched by CN- from the aqueous solution of $\text{K}_3[\text{Fe}(\text{CN})_6]$ (0.5 mM). Second, Au@CN- solution was treated with 100 μM PB precursors (FeCl_3 , $\text{K}_4[\text{Fe}(\text{CN})_6]$), PB precursors were simultaneous added at the rate of 2 mL/h under vigorous stirring. The reactor was still placed in the room temperature and maintained for 3 h to obtain Au@PB NPs. The obtained Au@PB NPs mixture were treated with centrifugation 3500 rpm during 30 min, residual raw materials were removed by centrifugation with washed several times using water, then restored at 4°C.

Synthesis of Au@PB@HA NPs. Before synthesis of Au@PB@HA NPs, the above as-synthesized Au@PB NPs were filtered through a 200 nm membrane to remove their large aggregates, and then the Au@PB NPs were re-dispersed in 20 mL of water. Poly-L-lysine (PLL) played as a bridge role for grafting HA into Au@PB NPs, of which PLL could coat on the surface of Au@PB NPs by electrostatic interaction as well as react efficiently with HA with the help of EDC/NHS. Typically, the above Au@PB NPs were mixed with 0.6 % PLL and stirred at room temperature for 30 min. Then, the solution was centrifuged at 3000 rpm for 25 min, and the obtained NPs were washed with water for 3 times. Next, 1 mL of EDC (5 mg/mL in distilled water) and 1 mL of NHS (4 mg/mL in distilled water) were added into the above redispersed Au@PB@PLL with gentle stirring for 30 mins at room temperature. Then, 1 mL of 2 mg/mL HA aqueous solution was added into the mixture, stirring for 2 h at room temperature. Finally, the as-prepared Au@PB@HA NPs were centrifuged at 3000 rpm for 25 min, washed several times with de-ionized water, and then Au@PB@HA NPs were filtered through a 200 nm membrane to remove large aggregates, and the obtained Au@PB@HA dispersions were stored at 4 °C for further use.

Characterization. Fourier transform infrared (FTIR) spectra were collected on NICOLET 5700 FTIR Spectrometer (USA), all detected samples were dried by freeze drying, and pressed with KBr into compact chips. The crystallographic study of the Au@PB NPs was determined by X-ray diffraction (XRD, X'Pert Pro, Philips Corp. Nederland), using $\text{CuK}\alpha$ radiation at a scanning rate of 5°/min from 5° to 80°. X-ray photoelectron spectroscopy (XPS, Thermo Fisher Scientific ESCALAB 250Xi. USA), used for studying the components of the as-synthesized samples, which equipped with an Al $\text{K}\alpha$ ($h\nu=1486.6\text{eV}$) source and the X-ray spot size was 2.5 mm, all samples were dropped into a chip of silicon until natural drying. Transmission electron microscopy (TEM, JEM-2100 Japan) images of samples were obtained at an accelerating voltage of 200 kV, all samples were placed into carbon-supported film until natural drying. The stability and size distribution of the samples were measured by dynamic light scattering (DLS, Autosize LocFc-963, Malvern Instrument), and the zeta potentials were record as the same apparatus. UV-Vis spectra and Electron Spin Resonance (ESR) spectra were collected on a Lambda Bio 40 spectrophotometer (Perkin-Elmer) and a Bruker X-band spectrometer (A200), respectively. The gold concentrations in tissue and tumor were measured by inductively coupled plasma mass spectrometer (ICP-MS, PQ-MS. Germany).

SERS experiments. In order to test the SERS capability of Au@PB@HA NPs, SERS spectra of the as-prepared solutions were acquired using a confocal Raman microscope (Horiba, Japan) with a 785 nm excitation laser. Before measurement, the instrument was calibrated with a silicon standard whose Raman peak is centered at 520 cm^{-1} . Each sample was loaded into a glass capillary tube, tested parameters: a 10 \times (NA 0.4) microscope objective with a working distance of 10.6 mm and spot focused laser was used, the laser power was 10 mW and

acquisition time was 10 s per twice integration. Raman spectrum of living tumor cells and some traditional Raman active probes were measured as the above tested condition. Of which, traditional Raman active probes were chosen as rhodamine B, crystal violet, cresyl violet, and malachite green, they were dissolved into distilled water (10^{-7} M) and mixed with 1 ml Au NPs solution, then Stokes-shifted Raman spectra were obtained by Raman microscope. The cellular uptake of Au@PB NPs and Au@PB@HA NPs were studied by the SERS mapping function. The SERS mapping of 4T1 tumor cells with as-prepared probe was performed as following procedure. The 4T1 cells were seeded in 35-mm Petri dishes pre-incubated at 37°C under 5% CO₂. The cell culture medium in each well was then replaced by the as-synthesized probe containing culture medium with same concentrations (50 µg/mL). Afterwards, the cells were co-incubated with probe for intervals time and then washed with PBS (pH = 7.4) for several times, single cell was monitored by Raman mapping function, collecting Raman spectrum range from 1950 cm⁻¹ to 2400 cm⁻¹ with moving time of the x and y directions under a 50× (NA 0.5) objective lens. The intensity of the peak at 2156 cm⁻¹ was plotted to obtain the Raman imaging.

MR experiments. The MR weighted imaging of the samples in the different concentration was tested by a Siemens Magnetom Trio 3.0 T clinical MR scanner, longitudinal relaxation rates ($1/T_1$) and transverse relaxation rates ($1/T_2$) of the samples at varying Fe concentrations of Au@PB@HA NPs were calculated by MRI system. The parameters of the sample are as follows: TR = 400 ms, TE = 45 ms, FA = 176.57, matrix = 128 × 128, FOV = 4.0×4.0 cm², and slice thickness = 1 mm; TR = 2890 ms, TE = 140 ms, FA = 176.57, matrix = 128 × 128, FOV = 4.0×4.0 cm², and slice thickness = 1 mm.

In vitro PDT assay. The potential photodynamic effect of as-prepared materials was evaluated by electron paramagnetic resonance (EPR) spectroscopy, (EMX-6/1, Bruker, Karlsruhe, Germany). The spin-trapping reagent, 2,2,6,6-tetramethyl-4-piperidone (TMPD, 60 mM), was added to Au@PB@HA solution (200 µg/mL), and then the mixtures were illuminated at 808 nm laser (2.0 W/cm²) for 10 min, the laser-treated sample was immediately examined by EPR spectrometry using the following parameters: microwave power = 2.2 mW, modulation amplitude = 1 G, modulation frequency = 100 kHz, sweep width = 100 G, and scan rate = 1.62 Gs⁻¹. Beyond that, PB might trigger the decomposition of H₂O₂ to enhance the PDT effect, thus H₂O₂ was added to the above mixture as experimental groups. Control groups: sample without laser treatment. Meanwhile, UV-Vis spectroscopy of TMB was chosen as monitor for catalyzing H₂O₂. TMB was pre-dissolved in ethanol (1 mM), probe (200 µg/mL) was treated with TMB (20 µL), then treated with H₂O₂ (1 mM). The absorption spectra were recorded using UV-vis spectrophotometer.

In vitro photo-thermal test. The photo-thermal property of the as-prepared Au@PB@HA was investigated by a digital non-contact infrared thermometer. Aqueous solution containing samples (200 µg/mL) were transferred to a 1.5 mL plastic centrifuge tube and irradiated with an NIR laser (808 nm, 2.0 W) for 10 min, and the real time temperature was monitored every 30 s, photothermal images were acquired using a thermal camera at every 2 min after irradiation. The photothermal conversion efficiency (η) was calculated according to the following equation:

$$\eta = \frac{[(hA(I_{\max} - I_{\text{surr}}) - Q_{\text{dis}})]}{I(1 - 10^{-A\lambda})}$$

where h and A are the heat transfer coefficient and the surface area of the cuvette cell, respectively. T_{surr} and T_{max} are the initial and final temperatures of the solution. Q_{dis} represents the heat dissipation of the solvent (water) which was measured using a power meter (407A, Spectra-Physics). I is the incident laser power and Aλ is the absorbance at 808 nm. A dimensionless temperature driving force hA was calculated by the following equation:

$$hA = \frac{2mC_s}{\tau_s}$$

where m and C are the mass (1 g) and heat capacity (4.2 J/g) of water, respectively. τ_s is the sample system time constant calculated by the following equation:

$$\tau_s = -\frac{t}{\ln(\theta)}$$

where θ is the dimensionless driving force and t is time.

MTT test. The cytotoxicity was measured by performing methyl thiazolyl tetrazolium (MTT) assay on 4T1 cells. The 4T1 cells were seeded into 96 well culture plates (104 cells per well) pre-incubated at 37 °C under 5% CO₂. The cell culture medium in each well was then replaced by the as-synthesized probe containing culture medium with various concentrations (0-200 µg/mL). The cells were subsequently incubated for 24 h at 37 °C under 5% CO₂, and then washed with PBS (pH = 7.4) for several times. Afterward, 10 µL MTT (5 mg/mL in PBS solution) was added to each well and incubated for another 4 h. After removal of the growth medium, 200 µL DMSO was added to each well to completely dissolve the residual crystals. The optical density (OD) was measured in microplate reader at 570 nm. Cell viability was assessed by the formula:

$$\text{Relative Cell Viability (\%)} = \frac{\text{OD}_{\text{treated}} - \text{OD}_{\text{blank}}}{\text{OD}_{\text{control}} - \text{OD}_{\text{blank}}} \times 100\%$$

where $\text{OD}_{\text{treated}}$ corresponds to the absorbance of experimental cells treated with sample and $\text{OD}_{\text{control}}$ is the absorbance from control group without treatment. Three replicated experiments were performed for each concentration, and all processes were carried out in darkness.

Furthermore, the phototoxicity of Au@PB@HA to against 4T1 cells was visual detection by calcein acetoxymethyl ester (calcein AM) and propidium iodide (PI) staining. After exposed to laser for experiment group, 4T1 cells were stained with calcein AM and PI, the images were recorded by fluorescence microscope to visualize the effect of chemotherapy and photothermal therapy on the 4T1 cells.

Western blot. For evaluating the relationship between *in vivo* CD44 protein and as-prepared probes, western blotting analysis of the relative CD44 expression in tumor was assessed after injecting probes. In detail, mice bearing 4T1 tumors with a volume of about 300 mm³ were injected with saline, Au@PB NPs or Au@PB@HA NPs solution via the tail vein. After 12 h, the tumors were fetched, dissolved by RIPA buffer, and re-suspended in 50 μL of SDS buffer with 1 % β -mercaptoethanol. Subsequently, the lysated solutions were then heated for 5 min and separated by 10 % SDS-PAGE (15 μL per lane). After electrophoresis, the proteins were transferred to a PVDF membrane (Millipore) and the PVDF membranes were then blocked in PBS with 5 % skim milk for 1 h. Subsequently, the membranes were first incubated with the CD44 rabbit anti-mouse antibody (1:1000 dilution) overnight at 4 °C and then with the secondary antibody, HRP-goat antirabbit (1:10000 dilution, KPL), for 1 h. CD44 protein was monitored by enhanced chemiluminescence and GAPDH rabbit (Abcam, 1 : 10000 dilution) was employed as a protein loading control.

Animal model. Animal experiments were performed by the assistance with the Department of Radiology, Union Hospital, Huazhong University of Science and Technology, and all animal experiments followed the protocols of the Institutional Animal Care and Use Committee and were approved by the Institutional Animal Care and Use Committee at Huazhong University. All mice were obtained from the Experimental Animal Center of Tongji Medical College, Huazhong University of Science and Technology. For *in vivo* imaging, female BALB/c nude mice (adult, 5 weeks old) bearing 4T1 tumors were prepared by subcutaneous injection of 2×10^6 cells. Other experimental mice were all female BALB/c mice (adult, 5 weeks old), 4T1 tumors were generated on the back of each BALB/c mouse by subcutaneous injection of 2×10^6 cells, and when the tumors reached an approximate size of 120 mm³ the mice were used for the animal experiments.

***In vivo* imaging.** *In vivo* real-time T₁-T₂ weighed MR imaging was carried out on the same clinical apparatus (3.0 T) at different time points before and after intravenous injection of the samples via the tail vein (100 μL , 4 mg/mL). The mice were under anesthesia by pentobarbitalum natricum (1%) during the animal experiments. The relative signal intensity (*S*) of the tumors was calculated using the formula: $S = \frac{SI_{\text{post}}}{SI_{\text{pre}}} \times 100\%$.

In vivo SERS capacity was investigated as following process. After intravenous injection of the samples via the tail vein (100 μL , 4 mg/mL), Raman spectra were acquired at 785 nm (10 mW) with 50 s exposure time/five numbers acquisition per pixel. Raman images of removed edged solid tumor were obtained using the Raman point-mapping function by 785 nm laser with 10 s accumulation.

***In vivo* phototherapy.** For verifying phototherapy of as-synthesized materials to antitumor, the 4T1 tumor-bearing Balb/c mice were randomly assigned to five groups ($n = 3$ per group): (1) saline; (2) Laser; (3) Au@PB; (4) Au@PB after injection 12 h then treated 808-nm laser irradiation for 10 min; (5) Au@PB@HA after injection 8 h then treated 808-nm laser irradiation for 10 min; (6) Au@PB@HA after injection 12 h then treated 808-nm laser irradiation for 10 min. Experimental mice were injected with the same dose of samples (100 μL , 4 mg/mL). The length and width of each tumor was measured using a vernier caliper every day, and the tumor volume (*V*) was calculated as follows:

$$V = \frac{\text{length} \times \text{width}^2}{2}$$

Relative tumor volumes were calculated as V/V_0 , where V_0 is the original volume at 0 days. The body weight of each mouse was also recorded, and actual tumor weight in each group was recorded after 14 day.

Histological test. The tumors were harvested from mice in each group on the next day after intravenous injection and phototherapeutic treatment. All tissues were fixed in a 4% paraformaldehyde solution for 24 h, then they were processed routinely into paraffin and images of all the tissues stained with hematoxylin & eosin (H & E), and of slices of tumor stained with tunel, were observed by light microscopy (AMG EVOS XL Core, Life Technologies, USA).

Bio-distribution and blood analysis. Inductively coupled plasma mass spectrometer (ICP-MS) was used to determine the accumulation of the Au@PB@HA in the tumor and in the major tissues, such as the kidney, heart,

liver, spleen, lungs and brain. 4T1 tumor-bearing Balb/c mice after intravenous administration of the NPs (100 μ L, 4 mg/mL) via the tail vein, mice were sacrificed at 8 h and 12 h and their tissues were collected, weighed and solubilised in 5 mL mixed solutions ($\text{HNO}_3:\text{H}_2\text{O}_2 = 1:1$) overnight, and boiled for 2 h. After cooling down to room temperature, each of the resulting solutions was then diluted with distilled water to 10 mL, and subsequently analyzed by ICP-MS to determine the total amount of Au ions in each measured tissue. After that, 10 μ L blood were drawn from the tail vein of healthy Balb/c mice at different point intravenous injection of the NPs. The pyrolytic process was the same as above. The biodistribution in various organs of mice and blood clearance of these NPs were then calculated and plotted in units of % ID/g based on the following equation:

$$\text{Au (\% ID/g)} = \frac{\text{Au tissuelysate} \times V \text{ tissuelysate}}{\text{Au injected} \times V \text{ injected Au} \times \text{tissue weight} \times 100\%}$$

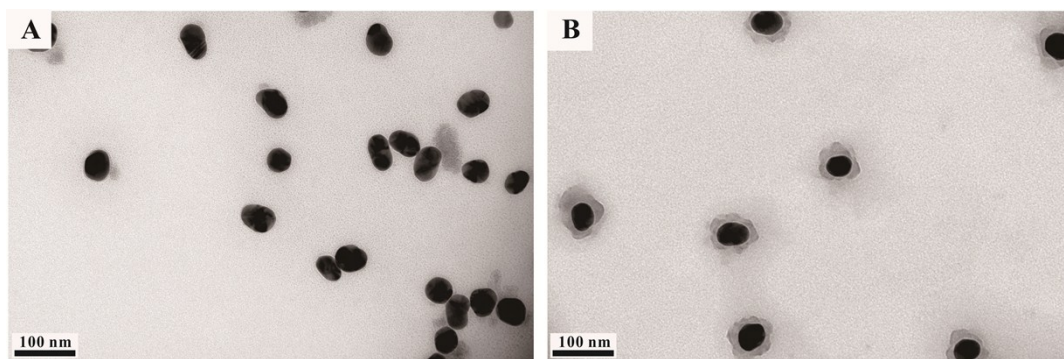


Fig. S1 TEM images of (A) Au@PB@HA NPs (Scale bar: 100 nm). (B) Au@PB NPs (Scale bar: 100 nm).

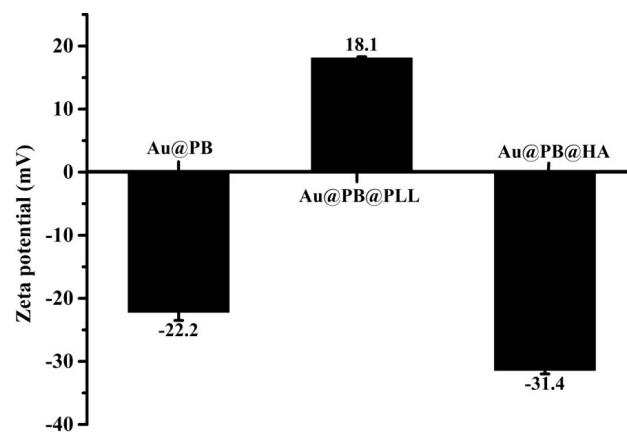


Fig. S2 Zeta potential of as synthesized NPs, such as Au@PB NPs, Au@PB@PLL NPs, and Au@PB@HA NPs, they were all dispersed into water for testing.

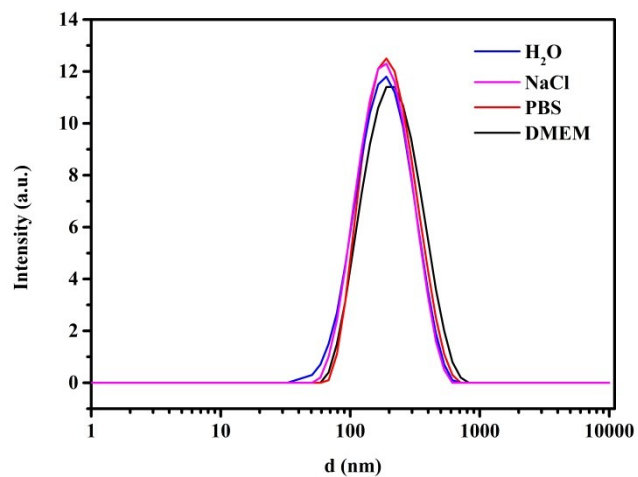


Fig. S3 Size stability of Au@PB@HA NPs, they were dispersed into several solvents, such as H₂O, NaCl (1 M), phosphate buffered solution (PBS), and cell culture solution DMEM, respectively.

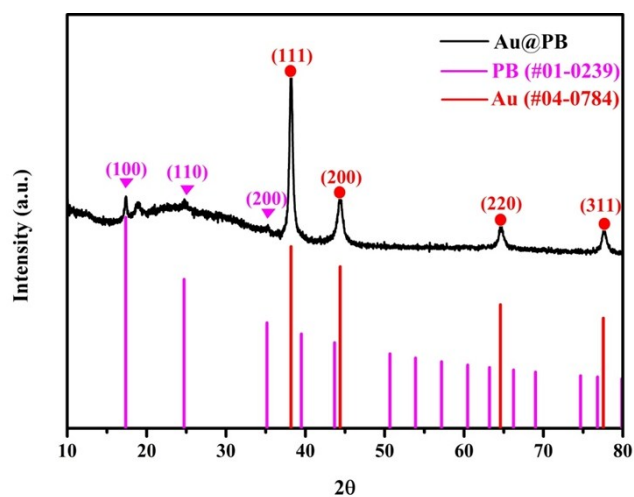


Fig. S4 XRD result of Au@PB NPs, cubic Au (JCPDS: 04-0784 pattern) and cubic PB (JPCD: 01-0239) as the main phases.

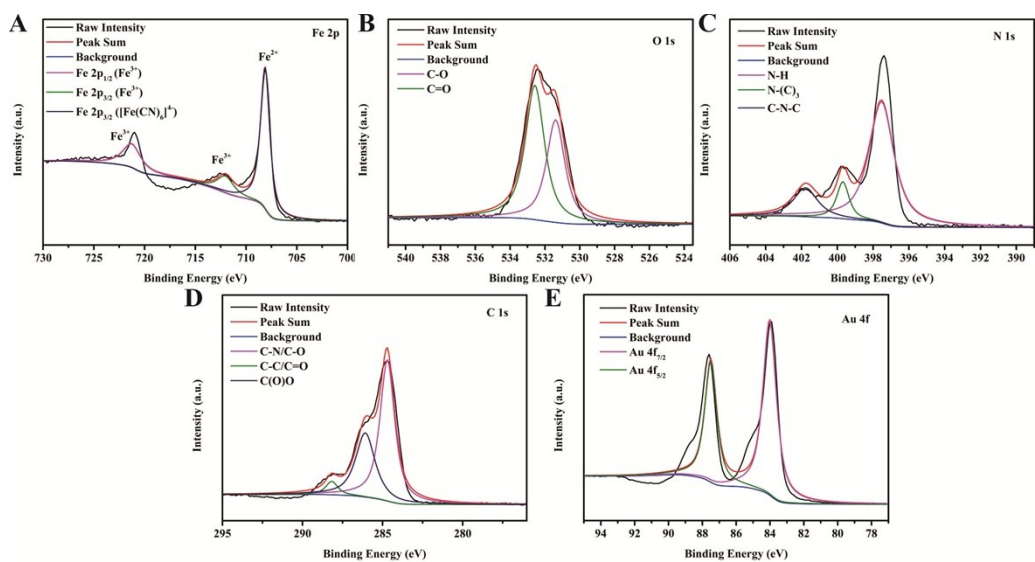


Fig. S5 XPS de-convoluted spectra of elements in Au@PB@HA NPs for (A) Fe 2p; (B) O 1s; (C) N 1s; (D) C 1s; (E) Au 4f.

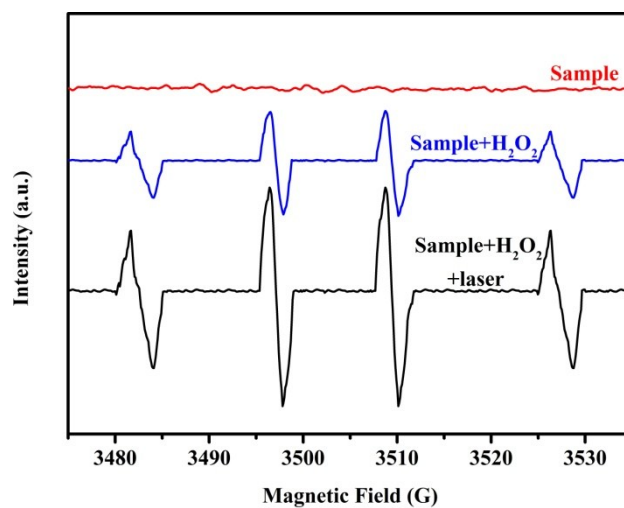


Fig. S6 EPR signal of $\cdot\text{OH}$ produced by Au@PB@HA NPs during photoirradiation using DMPO as a spin-trapping reagent. Sample: Au@PB@HA, [DMPO] = 80 mM, [H₂O₂] = 1 mM.

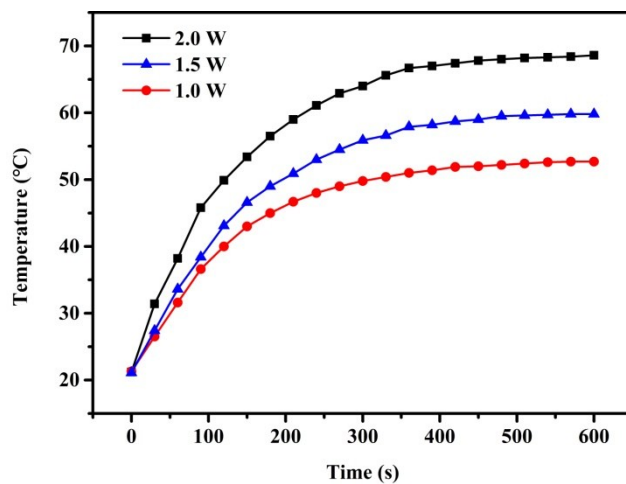


Fig. S7 Temperature change curve of Au@PB@HA solution (200 $\mu\text{g}/\text{mL}$) by 808 nm laser photoirradiation with changed laser powers.

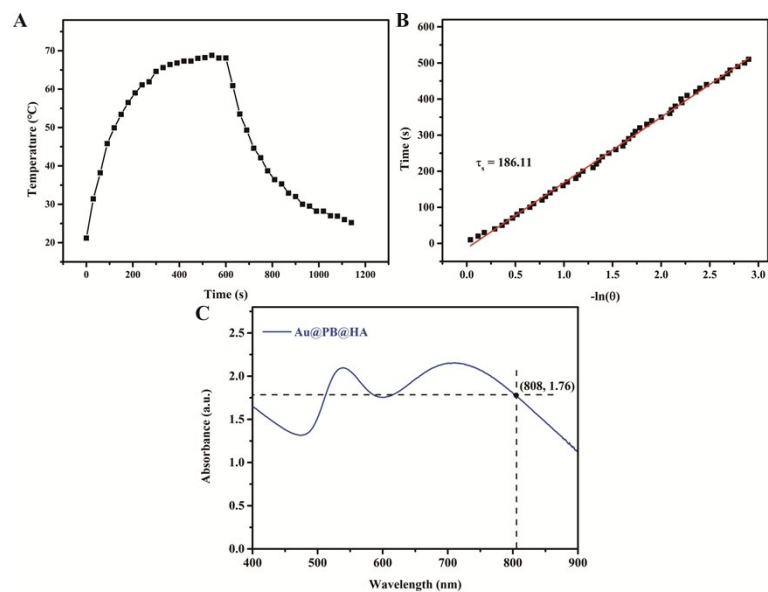


Fig. S8 (A) The corresponding time-dependent photothermal curves of Au@PB@HA NPs solution (200 $\mu\text{g}/\text{mL}$) during 808-nm laser ($2 \text{ W}/\text{cm}^2$) irradiation for 10 min, and turning off the laser for several min. (B) Time constant for heat transfer from the system is determined to be $\tau_s = 186.11$ s by applying the linear time data from the cooling period. (C) UV-Vis NIR absorption of Au@PB@HA NPs aqueous solution at the concentration of 200 $\mu\text{g}/\text{mL}$.

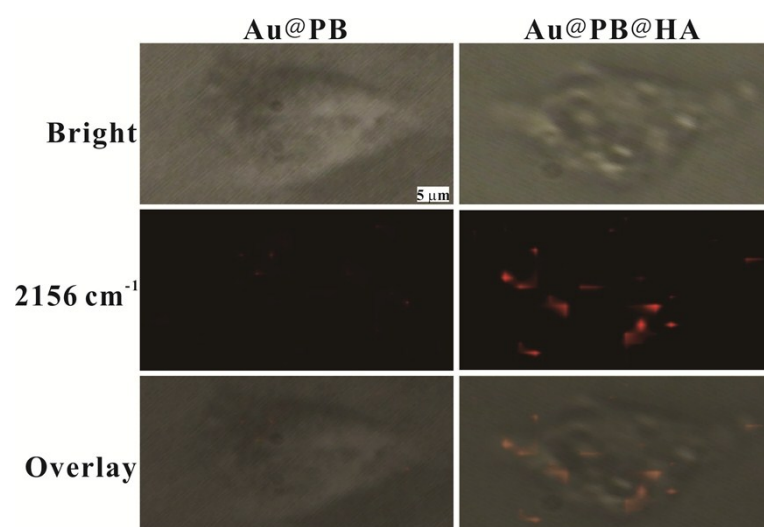


Fig. S9 Raman mapping of 4T1 cell after incubation with Au@PB and Au@PB@HA (50 μg/mL), red area represents Raman characteristic peak at 2156 cm⁻¹, scale bars: 5 μm.

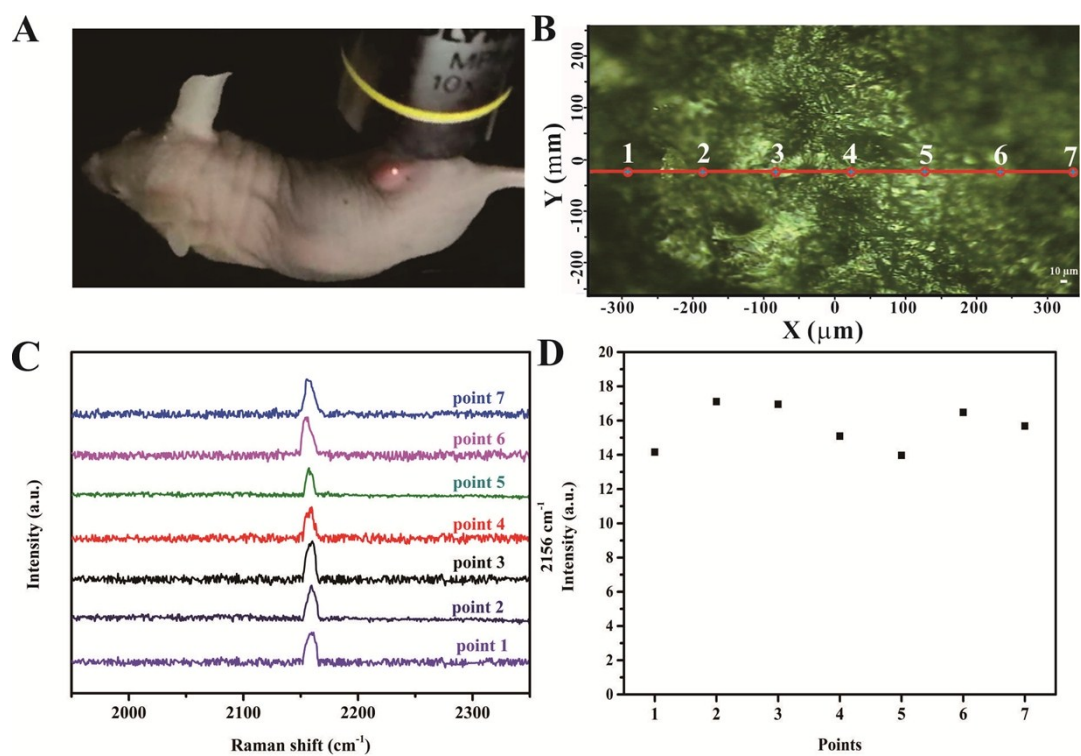


Fig. S 10 (A) Typical picture of a live mouse on the mobile platform under the SERS laser lens for detection. (B) Typical picture of partial tumor tissue in living mouse under 10 \times len, and the SERS detection positions are marked with red dots. (C) Representative Raman spectra at different points indicated in Fig. S11B. (D) Raman peak intensity of 2156 cm^{-1} obtained in the different positions of tumor site in living mouse.

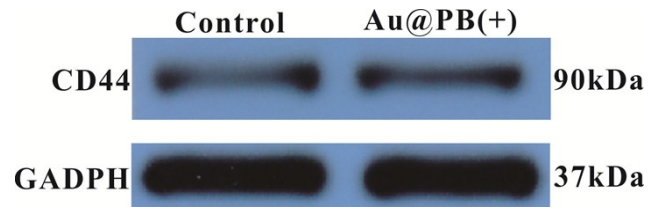


Fig. S11 Western blots of CD44 expression in 4T1 tumors treated with Au@PB.

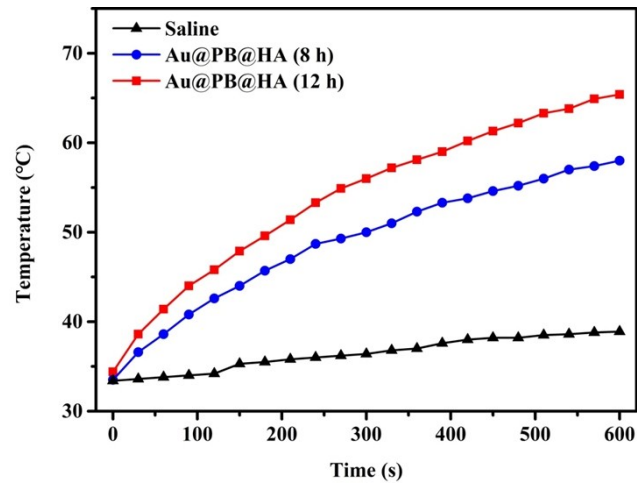


Fig. S12 Real time tumor temperature change during the irradiation time in each group, saline was the control group.

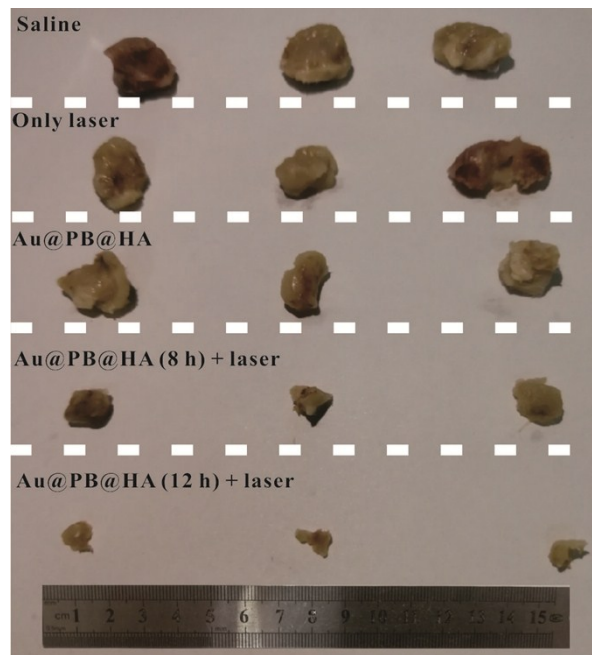


Fig. S13 Representative the tumor tissues collected from different groups at 14 days.

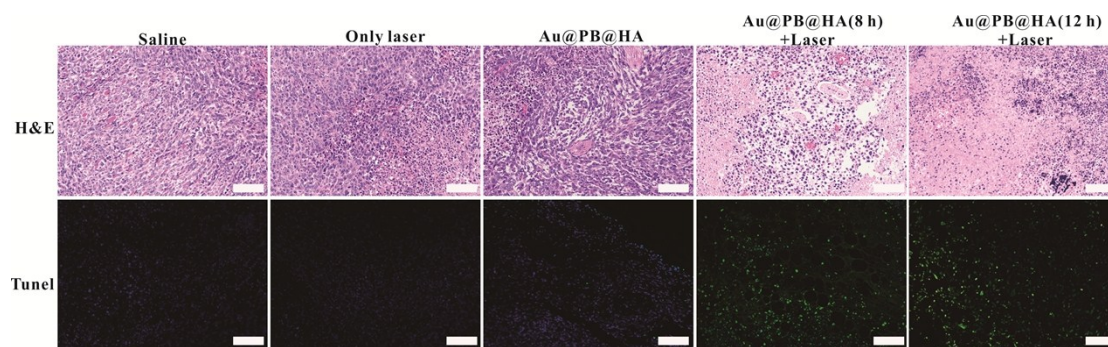


Fig. S14 Representative images of H&E and tunel fluorescence staining for tumor in the different groups. Scale bars: 100 μ m.

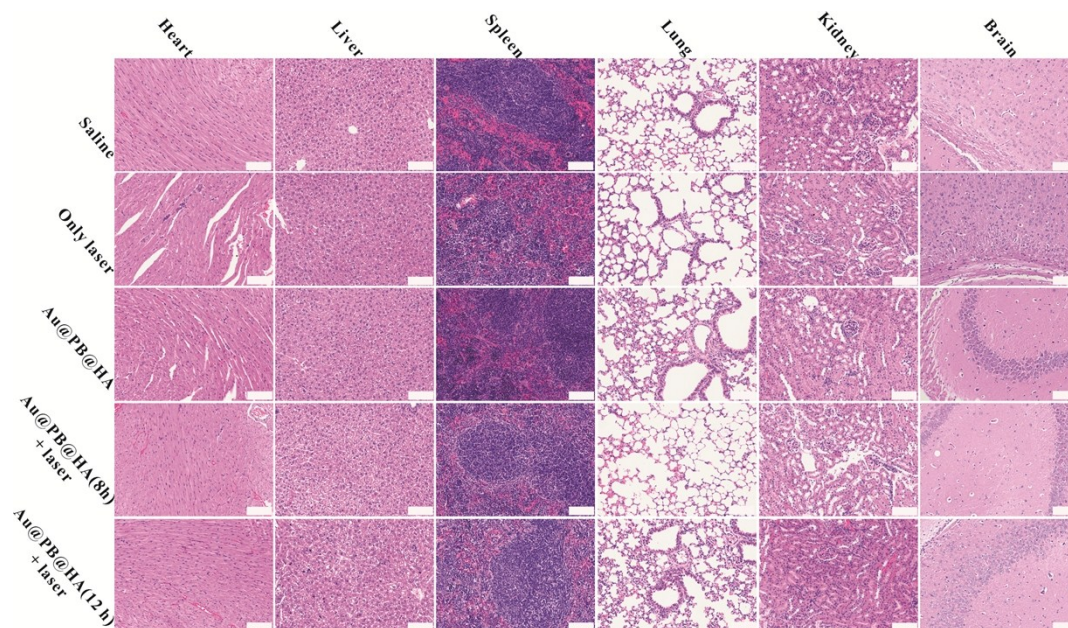


Fig. S15 H&E-stained histological section of spleen, liver, kidney, heart, lung tissues obtained from mice of the treatment. Scale bars: 200 µm.

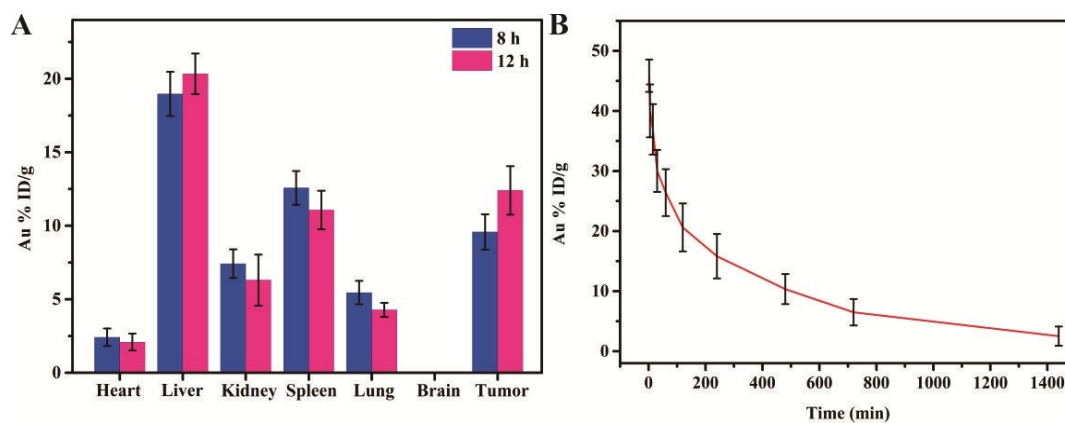


Fig. S16 (A) Concentration of the Au in organs and tumors at 8 h or 12 h after intravenous injection of the Au@PB@HA NPs. (B) Concentration of the Au in the blood at different time points after intravenous injection of the Au@PB@HA NPs. Error bars represent the standard deviation ($n = 3$).